Substituent Effects on the Thermal Cis-to-Trans Isomerization of 1,3-Diphenyltriazenes in Aqueous Solution

Nan Chen, Mónica Barra,* Ivan Lee, and Navjot Chahal

Department of Chemistry, University of Waterloo, Waterloo, Ontario, Canada N2L 3G1

mbarra@sciborg.uwaterloo.ca

Received November 21, 2001

The thermal cis-to-trans isomerization of some symmetrically *p*,*p*′-disubstituted 1,3-diphenyltriazenes has been studied by means of laser-flash photolysis techniques. The geometric isomerization is catalyzed by general acids and general bases as a result of acid/base-promoted 1,3-prototropic rearrangements. Acid catalysis becomes more prominent as the electron-donating character of the para substituent increases, while base catalysis becomes more important as the electron-withdrawing character of the para substituent increases. In addition, the rate ascribed to the interconversion of neutral cis rotamers through hindered rotation around the nitrogen−nitrogen single bond is found to decrease as the electron-withdrawing character of the para substituent increases. Rates of interconversion of neutral cis rotamers are also found to decrease with decreasing solvent polarity, which is indicative of the involvement of a polar transition state. On the other hand, kinetic investigations of the acid-catalyzed decomposition of target triazenes are consistent with an A1 mechanism.

Introduction

Triazenes, compounds characterized by having a diazoamino group (−N═N−N<), commonly adopt the trans configuration in the ground state. However, these compounds are also known to undergo reversible changes in double-bond configuration as a result of photoinduced and thermally induced trans−cis−trans isomerization.[1−4] Photochromic materials of this type are of interest for potential applications, among others, in molecular electronic devices.[5]

Previous work from our laboratory has shown that *cis*-1,3-diphenyltriazene (*cis*-**HDPT**), generated upon photoisomerization of *trans*-**HDPT** in 2% MeOH aqueous solutions at 6 < pH < 14, undergoes cis-to-trans isomerization catalyzed by general acids and general bases.[4] Acid catalysis is attributed to rate-limiting proton transfer to the diazo group, whereas base catalysis is attributed to rate-limiting base-promoted ionization of the amino nitrogen leading to geometric isomerization (Scheme 1). In addition, a process ascribed to the interconversion of cis rotamers through hindered rotation around the nitrogen−nitrogen single bond becomes rate-limiting at stronger basic conditions.[4]

The work described here focuses on the isomerization of some symmetrically *p*,*p*′-disubstituted 1,3-diphenyltriazenes (Chart 1) to further probe the isomerization mechanism reported and thus gain a better understanding of the rate-controlling factors. Substrate susceptibility to acid decomposition is also presented.

Scheme 1

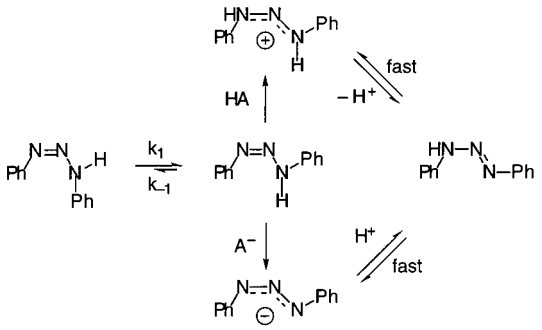

Chart 1

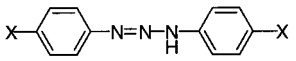

triazene	X
CH_3ODPT	CH_3O
CH_3DPT	CH_3
HDPT	H
ClDPT	Cl

triazene	X
CF_3DPT	CF_3
CNDPT	CN
NO_2DPT	NO_2

Results and Discussion

Acid-Catalyzed Decomposition. Due to the limited solubility of target triazenes in pure water, geometric isomerization studies were carried out in 30:70 (v/v) THF/water solutions, typically at pHs between 6 and 14. However, since it is well documented that triazenes are sensitive to the presence of acids,[6] to minimize substrate depletion while handling triazene aqueous solutions, a quantitative investigation of the stability of target sub-

(1) Le Fevre, R. J. W.; Liddicoet, T. H. *J. Chem. Soc.* **1951**, 2743.
(2) Baro, J.; Dudek, D.; Luther, K.; Troe, J. *Ber. Bunsen-Ges. Phys. Chem.* **1983**, *87*, 1155.
(3) Scaiano, J. C.; Chen, C.; McGarry, P. F. *J. Photochem. Photobiol. A: Chem.* **1991**, *62*, 75.
(4) Barra, M.; Chen, N. *J. Org. Chem.* **2000**, *65*, 5739.
(5) Martin, P. J. In *An Introduction to Molecular Electronics*; Petty, M. C., Bryce, M. R., Bloor, D., Eds.; Oxford University Press: New York, 1995; Chapter 6.
(6) Benson, F. R. *The High Nitrogen Compound*; John Wiley & Sons: New York, 1984; Chapter 6.

10.1021/jo011094d CCC: $22.00
Published on Web 03/13/2002

strates in the solvent employed in this study was also undertaken.

When the intensity corresponding to the longest-wavelength absorption band of target triazenes in acidic media is monitored as a function of time, a decrease in signal intensity is observed due to triazene decomposition. In all cases, the rate of the reactions follows first-order kinetics, and the corresponding observed rate constants (k_{obs}) are found to increase with proton concentration (Table S1).[7] The acid catalysis is interpreted in terms of an A1 mechanism (eq 1), in accordance with reports in the literature.[8−10] The corresponding expression for the observed rate constant is given by eq 2, where K_a, $k_{cleavage}$, and γ_{H+} represent, respectively, the acid dissociation equilibrium constant for the diazoammonium ion, the first-order rate constant for cleavage of the nitrogen−nitrogen single bond, and the activity coefficient for a proton.

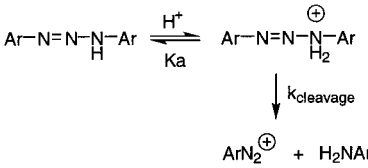

(1)

$$k_{obs} = \frac{k_{cleavage}[H^+]}{K_a + [H^+]} = \frac{k_{cleavage}10^{-pH}}{\gamma_{H+}K_a + 10^{-pH}} \qquad (2)$$

The linear dependence observed between k_{obs} and 10^{-pH} values (plots not shown) would indicate that, under the experimental conditions of this study, the factor $\gamma_{H+}K_a$ is at least 10 times larger than the highest 10^{-pH} value for each series studied; thus, the slope of the linear plots corresponds to the second-order rate coefficient $k_{cleavage}/(\gamma_{H+}K_a)$. Values for the latter (Table S2)[7] are displayed in Figure 1 (filled circles) vs the corresponding Hammett substituent constants.[11] Not surprisingly, triazene stability increases with increasing electron-withdrawing character of the para substituent; i.e., the basicity of the amino nitrogen and the stability of the diazonium ion intermediate both decrease with increasing electron-withdrawing character of the para substituent. It should be pointed out here that the slope value corresponding to Figure 1 (i.e., $\rho = -(3.1 \pm 0.1)$) is in excellent agreement with reaction constants determined for acid-catalyzed decomposition of similar systems, e.g., disubstituted 1,3-diphenyltriazenes −2.97[12] (20 °C, 20% aqueous ethanol),[9] disubstituted 3-(*N*-methylcarbamoyl)-1,3-diphenyltriazenes −2.39 (25 °C, water),[13] and 1-substituted 1,3-diphenyl-3-methyltriazenes −3.70 (25 °C, 40% aqueous ethanol).[10]

Thermal Cis−Trans Isomerization. Laser excitation (355 nm) of any of the target triazenes in buffered

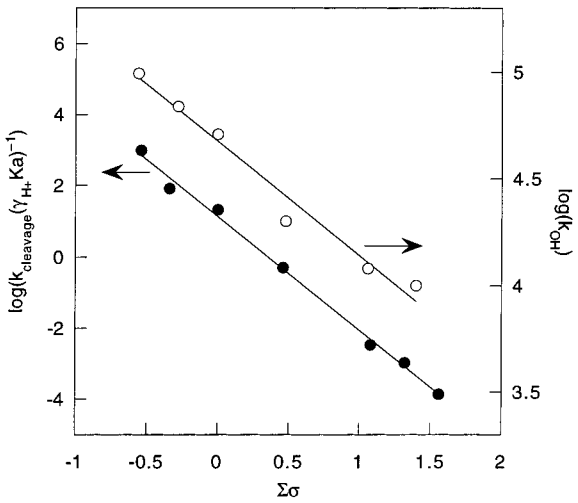

Figure 1. Hammett dependence of the second-order rate coefficient for acid-catalyzed decomposition (●) and of the observed rate constant for cis-to-trans isomerization in NaOH solutions (○) of symmetrically *p,p′*-disubstituted 1,3-diphenyltriazenes.

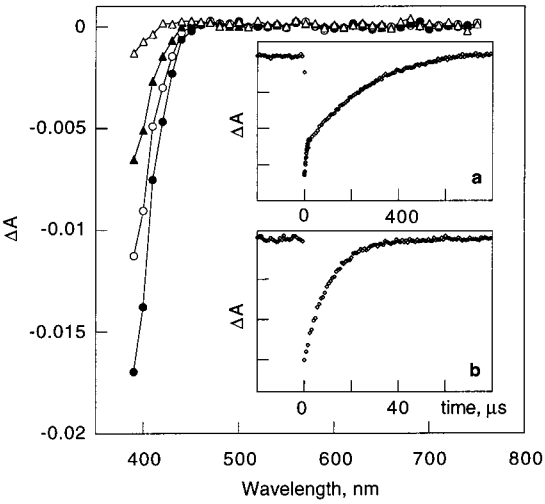

Figure 2. Transient absorption spectra for **CH_3ODPT** (in 0.05 M NaOH solution) obtained 3.2 (●), 8.4 (○), 16 (▲), and 71.2 μs (△) after laser pulse. Inset: kinetic traces recorded at 390 nm at (a) pH = 6.80 (0.01 M phosphate buffer) and (b) 0.197 M NaOH solution.

30:70 (v/v) THF/water solutions leads to negative changes in absorbance (bleaching), followed by complete recovery of the initial absorbance of the solutions (e.g., Figure 2). The resulting transient absorption spectra are in fact mirror images of the corresponding ground-state absorption spectra (e.g., Figure 3). It is noticed that the shape of these spectra is pH dependent only in the case of **XDPT** having electron-withdrawing substituents, i.e., X = Cl, CF_3, CN, and NO_2 (e.g., Figures 3 and 4). These pH-dependent spectral changes are consistent with changes in the relative concentrations of neutral trans triazene and of its conjugate anionic form, as would be expected under the experimental conditions of this work (i.e., 6 < pH < 14) by taking into account the corresponding pK_a^{trans} value for deprotonation of the amino nitrogen (Table 1). In all cases, the absorption band corresponding to the anionic trans form is red-shifted with respect to that of its conjugate neutral form.

(7) Supporting Information: see paragraph at the end of this paper regarding availability.

(8) Zverina, V.; Remes, M.; Divis, J.; Marhold, J.; Matrka, M. *Collec. Czech. Chem. Commun.* **1973**, *38*, 251.

(9) Benes, J.; Beranek, V.; Zimprich, J.; Veternik, P. *Collec. Czech. Chem. Commun.* **1977**, *42*, 702.

(10) Svoboda, P.; Pytela, O.; Vecera, M. *Collec. Czech. Chem. Commun.* **1986**, *51*, 553.

(11) March, J. *Advanced Organic Chemistry*; John Wiley & Sons: New York, 1992; p 280.

(12) Reaction constant for Hammett relation in the Yukawa−Tsuno modification.

(13) Pytela, O.; Vecera, M.; Vetesnik, P. *Collec. Czech. Chem. Commun.* **1980**, *45*, 2108.

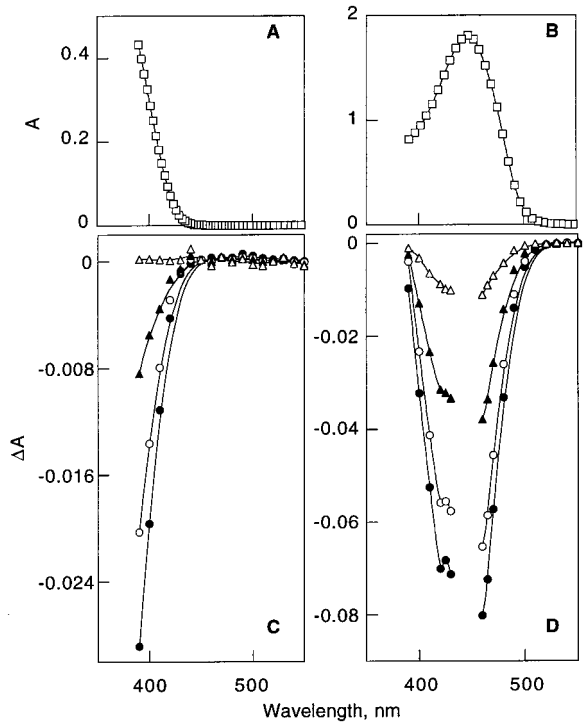

Figure 3. Ground-state absorption spectra for *trans*-**CNDPT** at pH = 6.30 (A) and 11.02 (B). Transient absorption spectra for **CNDPT** obtained at pH = 6.30 (0.05 M phosphate buffer) 36 (●), 140 (○), 344 (▲), and 728 μs (△) after laser pulse (C) and at pH = 11.02 (0.05 M carbonate buffer) 3.2 (●), 24 (○), 69.6 (▲), and 146 μs (△) after laser pulse (D).

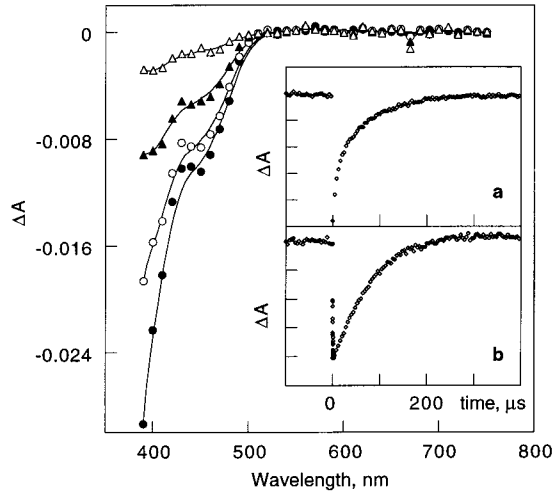

Figure 4. Transient absorption spectra for **CNDPT** at pH = 9.62 (0.05 M carbonate buffer) obtained 7.2 (●), 28 (○), 68.8 (▲), and 146 μs (△) after laser pulse. Inset: kinetic traces recorded at pH = 9.62 (0.1 M carbonate buffer) at (a) 390 and (b) 445 nm.

In the case of **XDPT** with X = CH_3O, CH_3, H, and Cl, bleaching is instantaneous at all pHs (e.g., Figure 2 inset). However, in the case of **XDPT** with X = CF_3, CN, and NO_2, in addition to instantaneous bleaching, a time-resolved bleaching (e.g., Figure 4, inset b) can also be observed at pH $\approx$ $pK_a^{trans} \pm 1$. In all cases, the instantaneous bleaching is ascribed to photoinduced trans-to-cis isomerization, consistent with previous studies on **HDPT**,[3,4] the compound for which the cis isomer has been shown to have a lower absorptivity at $\lambda > 350$ nm with respect to the trans form.[14] On the other hand, the time-resolved bleaching detected with the most acidic triazenes is only observed in the spectral region corresponding to the absorption band of the anionic trans form, and it is ascribed to the acid/base equilibrium of the ground-state trans isomer due to the preferential photoinduced trans-to-cis isomerization of the neutral form (vide infra).

Table 1. Equilibrium Constants for Deprotonation of the Amino Nitrogen of *trans*-XDPT and Average Values for the Observed Rate Constants for Interconversion of *cis*-XDPT Rotamers in Aqueous Solution[a]

X	pK_a^{trans} [b]	$k^f_{average}$, 10^4 s^{-1}	k_{OH}, 10^4 s^{-1}
CH_3O		10.8 ± 0.8	9.9 ± 0.4
CH_3		7.7 ± 0.6	6.9 ± 0.2
H	>14	6.4 ± 0.6	5.1 ± 0.2
Cl	13.2 ± 0.1	2.3 ± 0.4	1.8 ± 0.1
CF_3	11.71 ± 0.05		1.2 ± 0.1
CN	10.52 ± 0.02		1.0 ± 0.1[c]
NO_2	9.46 ± 0.04		

[a] Solvent contains 30% THF, μ = 0.5 M (NaCl), T = 21 °C. [b] Determined spectrophotometrically. [c] Determined by curve fitting from data in Figure 7; see text.

The complete recovery of the initial absorbance of the solutions clearly indicates that the geometric isomerization is reversible in all cases. Recovery traces were collected as a function of pH and of total buffer concentration. Results obtained using **XDPT** with X = CH_3O, CH_3, H, and Cl are overall very similar to those of our previous study on **HDPT** in 2% MeOH aqueous solutions:[4] (a) at any given pH and buffer concentration, kinetic traces do not vary with monitoring wavelength ($\lambda_{monitoring}$); (b) recovery traces are fitted to one or two exponential terms (depending on the pH); (c) when two first-order processes are detected (typically at pH < 10), the observed rate constant corresponding to the faster process (k_{obs}^f) is independent of pH and buffer concentration (Tables S3, S6, S9, and S12),[7] while the observed rate constant for the slower process (k_{obs}^s) varies with pH and buffer concentration (Tables S4, S7, S10, and S13);[7] (d) the preexponential factors corresponding to the two first-order processes just mentioned are independent of pH and buffer concentration; (e) only one first-order process, which is independent of pH, is observed in NaOH solutions (Tables, S5, S8, S11, and S14);[7] and (f) the average rate constant for the latter (k_{OH}) is in very good agreement with the corresponding k_{obs}^f average value obtained at lower pHs (Table 1). Furthermore, with any of these substrates, plots of k_{obs}^s vs buffer concentration are fairly linear, and data are interpreted in terms of eq 3,

$$k_{obs}^s = k_O + k_C[\text{buffer}] \qquad (3)$$

where k_C and k_O represent, respectively, the catalytic rate coefficient for the buffer species and the reaction through solvent-related species. In the case of data for phosphate buffer (i.e., pH < 8), values of k_C and k_O are found to decrease with increasing pH (Table 2), which is indicative of general acid catalysis, as illustrated in Figures 5A and 6 (diagonal portion of slope −1 of the V-shaped profile).[15] Despite the limited number of points, the clear nonlinear dependence of k_C on the molar fraction of free acid of

(14) Baro, J.; Dudek, D.; Luther, K.; Troe, J. *Ber. Bunsen-Ges. Phys. Chem.* **1983**, *87*, 1161.

(15) The slowest rate constant that can be determined with our laser-flash photolysis system is ca. 2000 s^{-1}.

Table 2. Catalytic Rate Coefficients (k_C) and Rate Constants for Reaction through Solvent-Related Species (k_O) for Cis−Trans Isomerization of Symmetrically *p,p′*-Disubstituted 1,3-Diphenyltriazenes in Aqueous Solution[a]

pH	k_C,[b] 10^4 M^{-1} s^{-1}	k_O,[b] 10^3 s^{-1}	pH	k_C,[b] 10^4 M^{-1} s^{-1}	k_O,[b] 10^3 s^{-1}	pH	k_C,[b] 10^4 M^{-1} s^{-1}	k_O,[b] 10^3 s^{-1}
CH_3ODPT			**HDPT**			**CF_3DPT**		
6.14[c]	15.4 ± 0.5	7.4 ± 0.3	6.04[c]	7 ± 1	9.4 ± 0.7	5.77[c]		3.1 ± 0.1
6.27[c]	11.7 ± 0.6	6.5 ± 0.4	6.27[c]	3.6 ± 0.6	6.4 ± 0.4	6.27[c]		3.0 ± 0.1
6.80[c]	6.9 ± 0.3	2.7 ± 0.2	6.80[c]	1.3 ± 0.3	2.8 ± 0.2	7.91[c]		2.9 ± 0.1
9.88[e]		5.8 ± 0.1	7.35[c]		2.4 ± 0.1	9.50[e]	0.7 ± 0.5	3.6 ± 0.2
10.28[e]	4.6 ± 0.9	8.7 ± 0.5	7.92[c]		1.9 ± 0.1[f]	9.94[e]	3.4 ± 0.5	5.0 ± 0.3
11.33[e]		65 ± 1	9.62[e]	0.8 ± 0.3	4.5 ± 0.2	10.97[e]		11.8 ± 0.1
CH_3DPT			9.79[e]	1.8 ± 0.3	6.1 ± 0.2	**CNDPT**		
6.14[c]	7.1 ± 0.4	7.1 ± 0.2	10.26[e]		19.4 ± 0.4	5.77[c]	0.48 ± 0.09	2.6 ± 0.1
6.26[c]	5.9 ± 0.4	5.5 ± 0.3	10.75[e]		23.5 ± 0.9	6.28[c]	0.53 ± 0.08	2.2 ± 0.1
6.81[c]	2.0 ± 0.2	3.0 ± 0.1	11.08[e]		44 ± 1	7.91[c]	2.3 ± 0.2	2.0 ± 0.1
9.89[e]	0.65 ± 0.20	4.3 ± 0.1	11.20[e]		49.7 ± 0.2	9.62[e]	3 ± 1	8.9 ± 0.7
10.35[e]		9.3 ± 0.3	**ClDPT**			10.26[e]		10.6 ± 0.1
11.33[e]		39 ± 1	5.74[c]	5 ± 1	8.5 ± 0.7	11.07[e]		11.3 ± 0.3
			6.01[c]	2.0 ± 0.6	5.4 ± 0.4	**NO_2DPT**		
			6.25[c]		4.4 ± 0.2	5.78[c]	0.8 ± 0.3	1.9 ± 0.2
			6.82[c]		2.50 ± 0.06	6.27[c]	1.7 ± 0.2	1.9 ± 0.1
			7.50[c]		2.16 ± 0.07[f]	7.91[c]	10 ± 1	2.3 ± 0.6
			7.74[c]		1.92 ± 0.05[f]	9.62[e]	31 ± 5	24 ± 3
			8.13[d]	1.0 ± 0.2	1.9 ± 0.2			
			9.64[e]	1.3 ± 0.6	5.8 ± 0.4			
			10.39[e]	4 ± 1	10 ± 1			

[a] Solvent contains 30% THF, μ = 0.5 M (NaCl), T = 21 °C. [b] Uncertainty corresponds to standard error. [c] Phosphate buffer. [d] Tris(hydroxymethyl)aminomethane buffer. [e] Carbonate buffer. [f] Observed value corresponds indeed to the response limit of our laser-flash photolysis system ($1/\tau$ ca. 2000 s^{-1}).

buffer component x_{HA} is attributed to acid catalysis by $H_2PO_4^-$ as well as by H_3PO_4, as previously reported.[4] Interestingly, at any given pH, the catalytic rate coefficient k_C diminishes as the electron-donating character of the para substituent also diminishes. On the other hand, in the case of data obtained at 8 < pH < 11 (i.e., tris(hydroxymethyl)aminomethane and carbonate buffers), values of k_C (if at all significant) and k_O (diagonal portion of slope +1 of the V-shaped profile of Figure 6) are found to increase with increasing pH (Table 2), which is indicative of general base catalysis. Furthermore, as illustrated in Figure 6 for **HDPT**, the downward bend observed at high pHs in the pH−rate profile is indicative of a change in rate-controlling step. All these observations are consistent with the reaction mechanism given in Scheme 1; i.e., the general acid/base catalysis being observed is attributed to acid/base-promoted 1,3-prototropic rearrangements leading to geometric isomerization, while the pH- and buffer-independent process is ascribed to the interconversion of neutral cis isomers. The latter process becomes rate-controlling typically at pH > 11. As shown in Figure 6 for **HDPT**, and from comparison of the values given in Table 1, $k^f_{average}$ seems to be larger than k_{OH}. The small difference between these two sets of values, if at all significant, might indicate that, under the experimental conditions of this study, both k_1 and k_{-1} should be considered; therefore, values of $k^f_{average}$ would correspond to ($k_1 + k_{-1}$), whereas values of k_{OH} would correspond to k_1.

It should be pointed out here that the preexponential factor corresponding to the faster first-order process observed typically at pH < 10 (ascribed to the interconversion of cis rotamers) diminishes as the electron-donating character of the para substituent decreases. For instance, in the case of **CH_3ODPT**, it represents 25% of the total signal, while in the case of **ClDPT**, it represents only 10%. This trend would indicate that the difference in absorptivity between the neutral cis rotamers at λ = 390 nm (the shortest $\lambda_{monitoring}$ of this study), the amount of the less stable cis rotamer generated upon photoexcitation, or the combination of these two factors diminishes with decreasing electron-donating character of the para

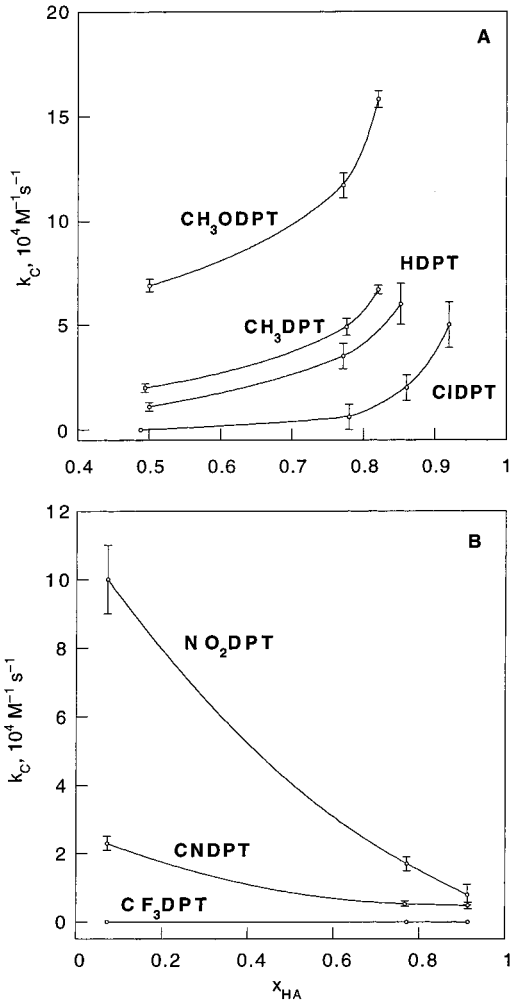

Figure 5. Plot of catalytic rate coefficients vs molar fraction of acid for cis-to-trans isomerization of *p,p′*-disubstituted 1,3-diphenyltriazenes in phosphate buffer.

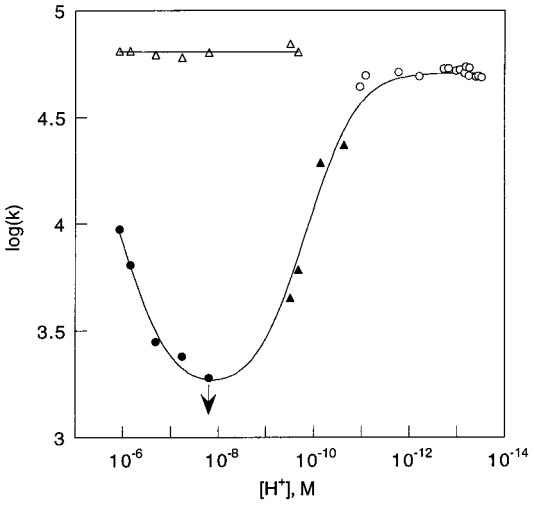

Figure 6. Rate profile for cis-to-trans isomerization of **HDPT** in aqueous solution: ● and ▲, rate constants for reaction through solvent-related species (obtained from the intercept of buffer dependence plots for phosphate and carbonate buffers, respectively); △, observed rate constants for the faster process observed at pH < 10 in phosphate and carbonate buffers; ○, observed rate constants for the single process detected in NaOH solutions. Arrow indicates direction of possible movement of point, which is a maximum value.[15]

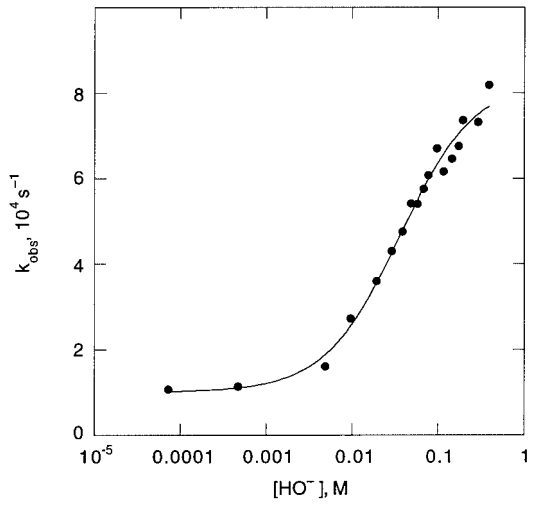

Figure 7. Plot of observed rate constants vs HO^- concentration for cis-to-trans isomerization of **CNDPT** in aqueous solutions at pH > 10.

substituent. Thus, it is not surprising to find that in the case of **CF_3DPT**, **CNDPT**, and **NO_2DPT**, recovery traces are very well reproduced by a single-exponential term.[16] The observed rate constants for cis-to-trans isomerization of these three substrates (Tables S15, S18, and S21)[7] increase with increasing buffer concentration and pH, consistent with general base catalysis. Plots of k_{obs} vs buffer concentration are fairly linear, and data are therefore interpreted in terms of eq 3 (Table 2). Interestingly, the catalytic rate coefficient k_C increases as the electron-withdrawing character of the para substituent also increases (e.g., Figure 5B). On the other hand, the first-order rate constants observed in NaOH solutions are pH independent in the case of **CF_3DPT** (Table S17),[7] while values for **CNDPT** (Table S20)[7] vary as shown in Figure 7; no signal could be observed in the case of **NO_2DPT** in solutions at pH > 10.

The amino nitrogen of *cis*-**XDPT** is expected to be less acidic than that in the corresponding trans isomeric form due to restricted resonance delocalization as a result of steric hindrance. This assumption is supported, for instance, by the differences in acidity reported for azo compounds such as 2-hydroxy-5-methylazobenzene ($pK_a^{trans} = 9.4$, $pK_a^{cis} = 10.7$)[17] and 4-[4′-(dimethylamino)-phenylazo]benzenesulfonate ($pK_a^{trans} = 2.70$[18]-2.87,[19] $pK_a^{cis} = 5.0$[20]). Thus, under the experimental conditions of this study (i.e., 6 < pH < 14), *trans*-**XDPT** with X = CH_3O, CH_3, and H (i.e., $pK_a^{trans} > 14$) exists in solution essentially in its neutral form, and therefore, laser excitation results in instantaneous formation of the corresponding neutral cis isomer. On the other hand, *trans*-**XDPT** with X = Cl, CF_3, CN, and NO_2 (i.e., $pK_a^{trans} < 14$) would also exist in its deprotonated form (depending on pH), and therefore, photoisomerization may lead to the formation of the corresponding neutral and/or anionic cis isomers. In the case of **XDPT** with X = CF_3, CN, and NO_2, photoisomerization of the neutral trans form seems to occur preferentially over the anionic form. This is inferred from the fact that when working at pH $\approx pK_a^{trans} \pm 1$, at the region where only the anionic trans form absorbs, not only is an instantaneous bleaching observed but also a time-resolved bleaching (e.g., Figure 4 inset b). The instantaneous bleaching, as already mentioned, corresponds to the photoinduced trans-to-cis isomerization, while the time-resolved bleaching is attributed to the acid/base equilibrium of the trans isomer as a result of the preferential removal of the neutral form upon photoisomerization. This interpretation is further supported by the fact that (a) the transient absorption spectra, recorded within the time frame corresponding to the time-resolved bleaching, are exact mirror images of the ground state absorption spectra, which includes a clearly defined isosbestic point (Figure 8) and (b) the rate constants for the time-resolved bleaching (Tables S16, S19, and S22)[7] are in excellent agreement with the values corresponding to the faster component of the recovery traces recorded under the same conditions at $\lambda_{monitoring}$ = 390 nm (λ at which the neutral trans form is the main absorbing species). As already mentioned, in the case of **NO_2DPT** no signal could be detected with solutions at pH > 10. The lack of signal probably indicates a low quantum yield for trans-to-cis isomerization of the anionic trans form. This assumption is consistent with the observation that under conditions where both the neutral and anionic *trans*-**NO_2DPT** forms are present in solution, no instantaneous bleaching can be observed in the region where the anionic trans form is the only absorbing species and only time-resolved bleaching is recorded (Figure 8 inset). Furthermore, it is noticed that for **CF_3DPT** and **CNDPT**, the contribution of the time-resolved bleaching relative to that of the instantaneous bleaching at pH $\approx pK_a^{trans}$ increases in the order **CF_3DPT** < **CNDPT**.

(16) At pH $\approx pK_a^{trans} \pm 1$, rate constants were obtained from kinetic traces collected at λ > 400 nm, where a time-resolved bleaching followed by signal recovery is observed; traces were reproduced by two well-separated exponential terms.

(17) Wettermark, G.; Langmuir, M. E.; Anderson, D. G. *J. Am. Chem. Soc.* **1965**, *87*, 476.
(18) Tawarah, K. M.; Abu-Shamleh, H. M. *Dyes and Pigments* **1991**, *16*, 241.
(19) Reeves, R. L. *J. Am. Chem. Soc.* **1966**, *88*, 2240.
(20) Sanchez, A. M.; Barra, M.; de Rossi, R. H. *J. Org. Chem.* **1999**, *64*, 1604.

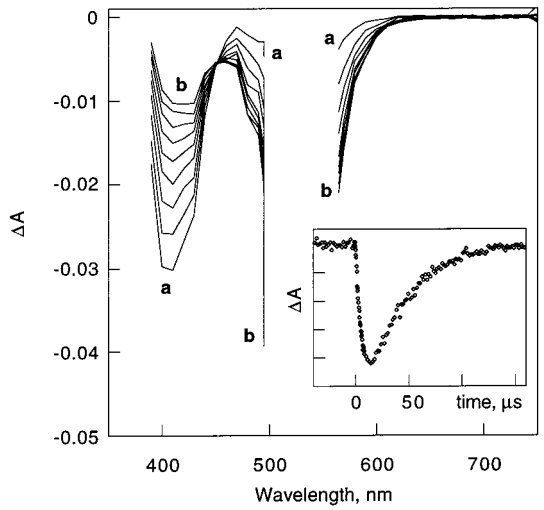

Figure 8. Transient absorption spectra for **NO_2DPT** at pH = 9.62 (0.05 M carbonate buffer) obtained within 0.2 and 3.4 μs (from a to b) after laser pulse. Inset: kinetic trace recorded at 570 nm (pH = 9.62, 0.01 M carbonate buffer).

Scheme 2

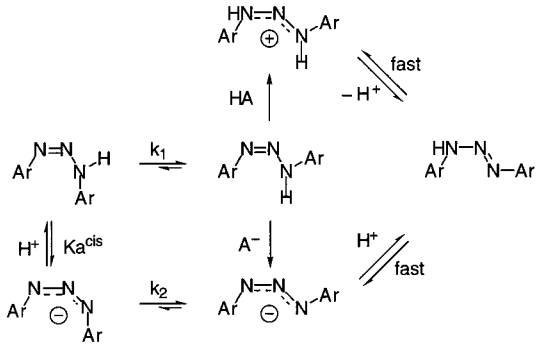

The pH dependence illustrated in Figure 7 is interpreted in terms of the reaction mechanism shown in Scheme 2; i.e., the observed rate constants in NaOH solutions would correspond to rate-limiting interconversion of conjugate rotamers of *cis*-**CNDPT** according to the rate law given by eq 4, in which k_1, k_2, and K_a^{cis} are defined as shown in Scheme 2 and K_w represents the equilibrium constant for self-ionization of water.

$$k_{obs} = \frac{k_1[H^+] + k_2K_a^{cis}}{[H^+] + K_a^{cis}} = \frac{k_1 + [HO^-]k_2K_a^{cis}/K_w}{1 + [HO^-]K_a^{cis}/K_w} \quad (4)$$

Curve fitting according to eq 4 leads to values of (1.0 $\pm$ 0.1) $\times$ 10^4 s^{-1}, (8 $\pm$ 2) $\times$ 10^4 s^{-1}, and 28 $\pm$ 3 for k_1, k_2, and K_a^{cis}/K_w, respectively; i.e., the anionic cis form of **CNDPT** isomerizes more rapidly than the neutral form, and the cis isomer is clearly less acidic than the trans form (since pK_w > 14 in 30% THF, then pK_a^{cis} > 12.6). As already mentioned, in the case of **CF_3DPT**, the observed rate constants in NaOH solutions are independent of pH; therefore, one must conclude either that pK_a^{cis} for **CF_3DPT** is significantly larger than 14 (fully consistent with the decrease in K_a of, at least, 2 orders of magnitude just described for *cis*-**CNDPT** (pK_a^{cis} > 12.6) vs *trans*-**CNDPT** (pK_a^{trans} = 10.52)) or, if indeed both conjugate forms of *cis*-**CF_3DPT** are present in solution, that $k_1 \approx k_2$.

Interestingly, comparison of the rate constants for interconversion of neutral cis rotamers (Table 1, k_{OH} = k_1) clearly shows that the reactivity diminishes as the electron-donating character of the para substituent diminishes as well. The Hammett plot represented in Figure 1 (open circles) is characterized by a ρ value of $-(0.53 \pm 0.04)$. Reported data for restricted rotation of *trans*-1-aryl-3,3-dialkyltriazenes in organic solvents lead to $\rho \approx -2$;[21-23] the restricted rotation around the nitrogen–nitrogen single bond of triazenes is ascribed to the partial double-bond character that results form 1,3-dipolar contributions as shown in eq 5.[21-27] Thus, the decrease in the rate for interconversion of neutral cis isomers with decreasing electron-donating character of the para substituent suggests predominant conjugation between the diazoamino group and the aromatic ring attached to the sp^2 nitrogen. This observation is also consistent with the increase in basicity of the amino nitrogen in the cis isomer relative to that in the trans form, as shown in the case of **CNDPT**, attributed to restricted conjugation between the amino nitrogen and the phenyl ring attached to it.

Table 3. Observed Rate Constants for Interconversion of Cis Rotamers in NaOH Aqueous Solutions as a Function of Organic Cosolvent[a]

	k_{OH}, 10^5 s^{-1} [b]			
	cosolvent			
triazene	CH_3OH	$(CH_3)_2SO$	CH_3CN	$(CH_3)_2CHOH$
CH_3ODPT	4.4 $\pm$ 0.1	2.94 $\pm$ 0.08	2.8 $\pm$ 0.1	2.54 $\pm$ 0.08
CH_3DPT	3.7 $\pm$ 0.1	2.5 $\pm$ 0.1	2.16 $\pm$ 0.07	1.89 $\pm$ 0.04
HDPT	3.4 $\pm$ 0.2	1.94 $\pm$ 0.09	1.62 $\pm$ 0.04	1.59 $\pm$ 0.06

[a] Solvent contains 30% organic cosolvent, μ = 0.5 M (NaCl), T = 21 °C. [b] Values correspond to the average of 5 independent experiments.

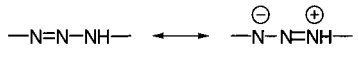

(5)

We noticed that the value of k_1 previously reported for **HDPT** in 2% MeOH, namely, (3.39 $\pm$ 0.05) $\times$ 10^5 s^{-1},[4] is significantly higher than the one presented here for **HDPT** in 30% THF. Thus, rate constants ascribed to the interconversion of neutral cis rotamers were also determined in NaOH solutions as a function of the nature and concentration of organic cosolvent. Rate constants are found to decrease (a) as the polarity and hydrogen bonding ability of the corresponding organic cosolvent decrease (Tables 3 and 4, last row) and (b) as the percentage of THF increases (Table 4). These results clearly indicate the involvement of a polar transition state.

In summary, the thermal cis-to-trans isomerization of symmetrically *p*,*p*′-disubstituted 1,3-diphenyltriazenes is catalyzed by general acids and general bases. Catalytic rate coefficients increase as the pK_a difference between

(21) Marullo, N. P.; Mayfield, C. B.; Wagener, E. H. *J. Am. Chem. Soc.* **1968**, *90*, 510.
(22) Akhtar, M. H.; McDaniel, R. S.; Feser, M.; Oehlschlager, A. C. *Tetrahedron* **1968**, *24*, 3899.
(23) Lippert, Th.; Wokaun, A.; Dauth, J.; Nuyken, O. *Magn. Reson. Chem.* **1992**, *30*, 1178.
(24) Lunazzi, L.; Cerioni, G.; Foresti, E.; Macciantelli, D. *J. Chem. Soc., Perkin Trans. 2* **1978**, 686.
(25) Sieh, D. H.; Wilbur, D. J.; Michejda, C. J. *J. Am. Chem. Soc.* **1980**, *102*, 3883.
(26) Golding, B. T.; Kemp, T. J.; Narayanaswamy, R.; Waters, B. W. *J. Chem. Res., Synop.* **1984**, 130.
(27) Panitz, J.-C.; Lippert, Th.; Stebani, J.; Nuyken, O.; Wokaun, A. *J. Phys. Chem.* **1993**, *97*, 5246.

Table 4. Observed Rate Constants for Interconversion of cis Rotamers in NaOH Aqueous Solutions as a Function of THF Concentration[a]

% THF (v/v)	k_{OH}, 10^5 s^{-1} [b]			
	CH_3ODPT	**CH_3DPT**	**HDPT**	**CF_3DPT**
5	4.6 ± 0.1	c	3.3 ± 0.1[d]	
10	4.28 ± 0.06	c	2.7 ± 0.2	0.32 ± 0.03
20	2.12 ± 0.07	1.52 ± 0.04	1.26 ± 0.08	0.174 ± 0.006
30	1.00 ± 0.03	0.66 ± 0.02	0.56 ± 0.02	0.098 ± 0.006

[a] μ = 0.5 M (NaCl), T = 21 °C. [b] Values correspond to the average of 5 independent experiments. [c] Measurements could not be performed due to the low solubility of the triazene. [d] 2% THF.

the triazene and the Brönsted catalyst also increases. Thus, acid catalysis becomes more prominent as the electron-donating character of the para substituent increases (e.g., Figure 5A), whereas base catalysis becomes more important as the electron-withdrawing character of the para substituent increases (e.g., Figure 5B). In all cases, interconversion of cis rotamers becomes rate controlling at high pHs. Interestingly, the rate for interconversion of neutral cis isomers decreases as the electron-withdrawing character of the para substituent increases, which suggests predominant conjugation between the diazo group and the phenyl ring attached to it; this conclusion is in agreement with the expected increase in pK_a^{cis} relative to pK_a^{trans}, as indeed observed in the case of **CNDPT**.

Experimental Section

1,3-Diphenyltriazene (Aldrich) was purified by treatment with $Cd(OH)_2$ generated in situ from $Cd(NO_3)_2$ (Allied Chemical) in basic methanol (BDH, ACS grade) aqueous solution, as described in the literature.[28] Symmetrically *p*,*p*′-disubstituted 1,3-diphenyltriazenes were synthesized by means of aniline/diazonium salts coupling via the classical diazotization method with $NaNO_2$[29] (X = NO_2) or using isoamyl nitrite[30] (X = CH_3O, CH_3) or sodium hexanitrocobaltate(III)[31] (X = Cl, CF_3, CN), as described in the literature. All *p*,*p*′-disubstituted 1,3-diphenyltriazenes were purified by recrystallization (Table S25);[7] melting points and ^{1}H NMR data (Table S25)[7] are in very good agreement with reported values.

Kinetic studies were carried out using 30:70 (v/v) THF/water as the solvent (unless stated otherwise). Aqueous buffers were prepared using analytical-grade salts, water purified in a Millipore apparatus, and spectrophotometric-grade organic solvents (BDH, Omnisolv grade). The ionic strength of the solutions was kept constant at 0.5 M using NaCl as a compensating electrolyte. The pH of these solutions was measured using a combination electrode that had been calibrated with standard aqueous buffers.

Acid dissociation equilibrium constants for deprotonation of the amino nitrogen of target triazenes were determined by the classical spectrophotometric method, by measuring the changes in absorbance at the wavelength of maximum absorption of each conjugate species as a function of pH; resulting values are in very good agreement with literature data for similar systems.[9]

Acid-catalyzed decomposition reactions were carried out under pseudo-first-order conditions and followed until at least 80−90% conversion of the starting material was observed. Typical substrate concentrations were in the order of (1−6) × 10^{-5} M. Rates of reaction were determined from the change in absorbance at the wavelength of maximum absorption of each target triazene (i.e., **CH_3ODPT** = 370 nm, **CH_3DPT** = 362 nm, **HDPT** = 365 nm, **ClDPT** = 363 nm, **CF_3DPT** = 357 nm, **CNDPT** = 372 nm, and **NO_2DPT** = 406 nm) as a function of time.

Laser experiments were carried out using a Q-switched Nd:YAG laser (Continuum, Surelite I) operated at 355 nm (4−6 ns pulses, <30 mJ/pulse) for excitation. Further details on this laser system have been reported elsewhere.[20] Solutions were contained in quartz cells constructed of 7 × 7 mm^2 Suprasil tubing. Transient absorption spectra were collected under flow conditions in order to ensure the irradiation of fresh portions of sample by each laser pulse. For each solution, kinetic traces were recorded at different time domains (typically between 0.08 and 8 μs/point) and then combined for analysis; if at all necessary, traces were previously normalized to account for slight differences in signal intensity due to laser power fluctuations. All measurements were carried out at 21 ± 1 °C.

All observed rate constants were determined by using the general curve-fitting procedure of Kaleidagraph 3.0.5 software from Abelbeck Software.

Molar fractions, such as those displayed in Figure 5, were calculated from the observed pH by using the ionization equilibrium constant for the corresponding buffer determined potentiometrically under our experimental conditions. Thus, ionization constants were obtained by extrapolating the pH values of solutions containing the corresponding conjugate acid and base in a 1:1 ratio to zero buffer concentration; resulting pK_a values are 6.76 ± 0.01 and 10.18 ± 0.01 for $H_2PO_4^-$ and HCO_3^-, respectively.

Acknowledgment. Financial support from the Natural Sciences and Engineering Research Council (NSERC) of Canada is gratefully acknowledged.

Supporting Information Available: Rate constants for acid-catalyzed decomposition and thermal cis−trans isomerization of symmetrically *p*,*p*′-disubstituted 1,3-diphenyltriazenes in buffered aqueous solutions as a function of pH and/or buffer concentration, as well as solvents for recrystallization, melting points, and ^{1}H NMR data of symmetrically *p*,*p*′-disubstituted 1,3-diphenyltriazenes synthesized. This material is available free of charge via the Internet at http://pubs.acs.org.

JO011094D

(28) Dwyer, F. P. *J. Chem. Soc. Ind., London* **1937**, *56T*, 70.
(29) Vogel, A. I. *Practical Organic Chemistry*; Longmans: New York, 1956; p 626.
(30) Vernin, G.; Siv, C.; Metzger, J. *Synthesis* **1977**, 691.
(31) Stefane, B.; Kocevar, M.; Polanc, S. *J. Org. Chem.* **1997**, *62*, 7165.